

Complex paths beyond Lefschetz thimbles: real time dynamics and the sign problem

Andrei Alexandru

Paulo Bedaque, Gökçe Başar, Neill Warrington, Greg Ridgway
Henry Lamm, Scott Lawrence

Quark Confinement and
Hadron Spectrum
August 2018



The plan

- Importance sampling and sign problem
- Complexification and contour deformation
- Generalized thimble method
- Case studies: Massive Thirring model & real-time correlators
- New proposals: sign optimized manifolds and learnifolds

Motivation

- Physical models of interest require non-perturbative calculations that have a sign problem:
 - QCD at finite baryon density (RHIC, neutron star structure, etc)
 - Real time dynamics for strongly coupled QFT
 - Strongly correlated electrons (Hubbard model, etc.)
- While a generic solution to the sign problem is impossible, thimble methods are likely to work for a large class of problems.

QFT on the lattice

- The partition function is expressed as a path integral
- The fields are sampled on a grid; differential operators are replaced by finite difference ones

$$Z = \int \mathcal{D}\phi e^{-S[\phi]} \rightarrow Z_{\text{latt}} = \int_{\mathbb{R}^N} \prod_i d\phi_i e^{-S[\phi]}$$
$$S_{\text{latt}} = \sum_n \left[\tilde{m} \phi_n^2 + \sum_{\alpha} \kappa_{\alpha} \phi_n \phi_{n+\hat{\alpha}} + \tilde{\lambda} \phi_n^4 \right]$$

- The partition function is a many-dimensional integral over **real** variables
- The integrand has **no singularity** for both bosonic and fermionic theories

Monte-Carlo sampling

- QFT correlators are statistical averages

$$\langle O \rangle = \frac{1}{Z} \int \mathcal{D}\phi e^{-S(\phi)} O(\phi)$$

- Estimate using importance sampling

$$\langle O \rangle \approx \frac{1}{N} \sum_{i=1}^N O(\phi_i) \quad \{\phi_1, \dots, \phi_N\} \text{ with } P(\phi) = \frac{1}{Z} e^{-S(\phi)}$$

- Stochastic errors decrease with sample size

$$\sigma_O = \sqrt{\langle O^2 \rangle - \langle O \rangle^2} \propto \frac{1}{\sqrt{N}}$$

Sign problem

- When the partition function is not real direct Monte-Carlo sampling is not possible

- The usual workaround involves *reweighting*

$$Z_0 = \int \mathcal{D}\phi \left| e^{-S(\phi)} \right| = \int \mathcal{D}\phi e^{-S_R(\phi)}$$

$$\langle O(\phi) \rangle_Z = \frac{\langle O(\phi) e^{-iS_I(\phi)} \rangle_{Z_0}}{\langle e^{-iS_I(\phi)} \rangle_{Z_0}}$$

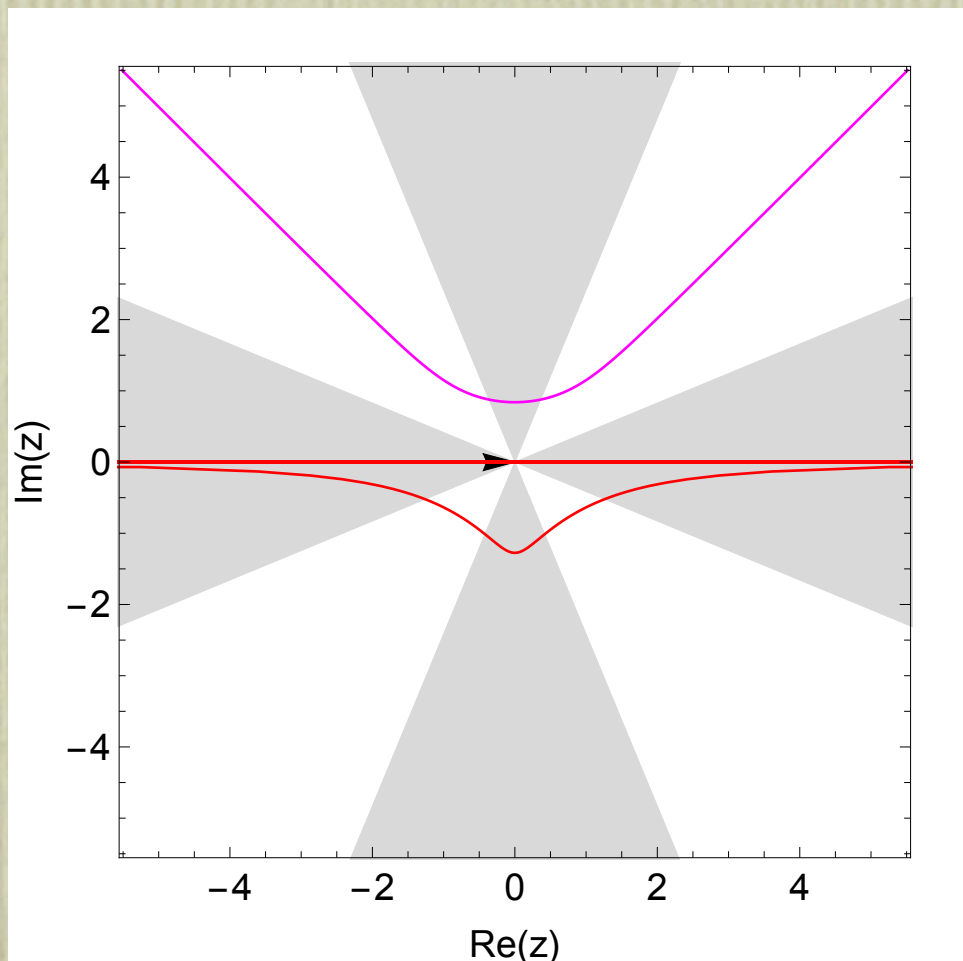
- Sampling is done based on S_R ; S_I is introduced in the observable: $\{\phi_1, \dots, \phi_N\}$ with $P(\phi) \propto e^{-S_R(\phi)}$

$$\langle O \rangle \approx \frac{1}{N} \sum_{i=1}^N O(\phi_i) e^{-iS_I(\phi)} \bigg/ \frac{1}{N} \sum_{i=1}^N e^{-iS_I(\phi)}$$

Sign problem

- A *sign problem* appears when the phase average is nearly zero (or zero): $e^{-iS_I(\phi_1)} + \dots + e^{-iS_I(\phi_N)} \ll N$
- The cost of the calculation is inversely proportional to the phase average: $N \propto \left\langle e^{-iS_I(\phi)} \right\rangle^{-2}$
- For example in QCD
$$\left\langle e^{-iS_I} \right\rangle_{Z_0} = \frac{Z}{Z_0} = e^{-\beta V(f_{\text{baryon}} - f_{\text{isospin}})} \rightarrow 0 \text{ as } V \rightarrow \infty$$
- In QCD the calculation cost increases exponentially with the volume

Contour deformation



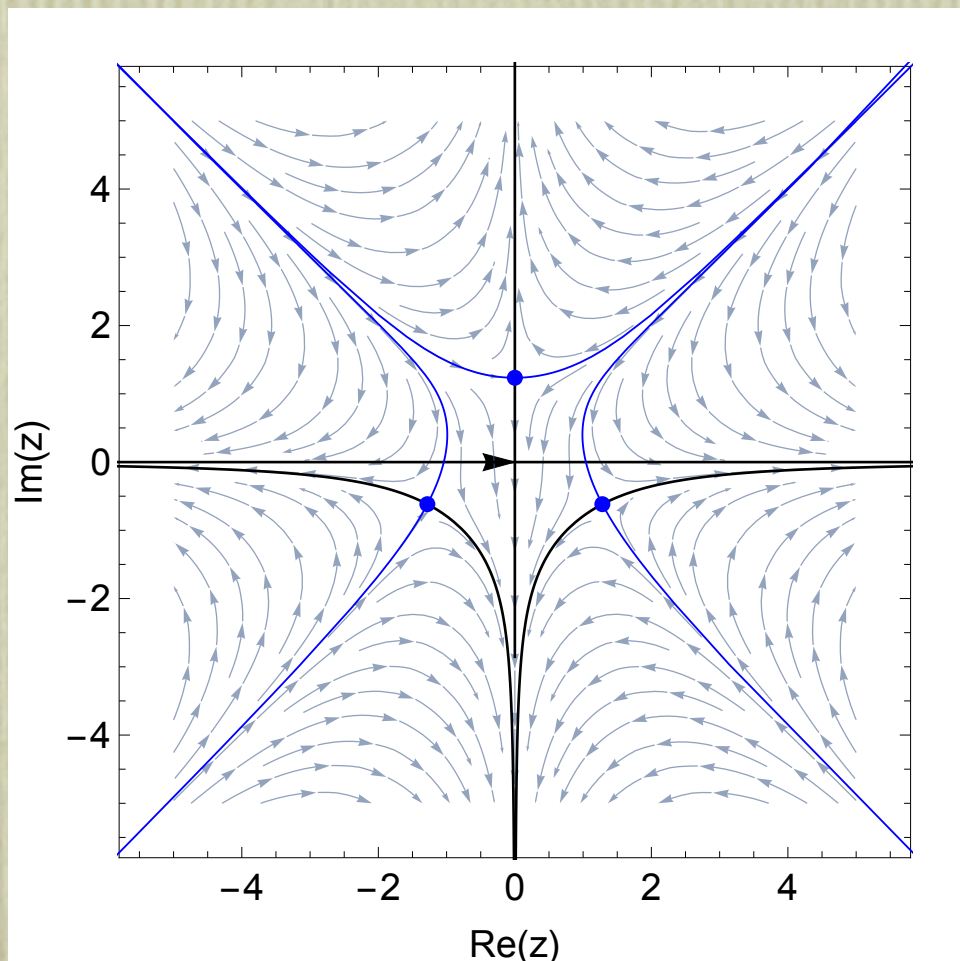
$$Z = \int_{-\infty}^{\infty} dx e^{-S(x)}$$

$$S(x) = x^4 - x^2 + 10ix$$

$$Z = \int_{\mathcal{C}} dz e^{-S(z)}$$

- Generalized Cauchy's theorem
- Deformation in the field variable space (lattice geometry unchanged)

Holomorphic gradient flow and Lefschetz thimbles



Thimbles are generalizations of steepest descent/stationary phase paths.

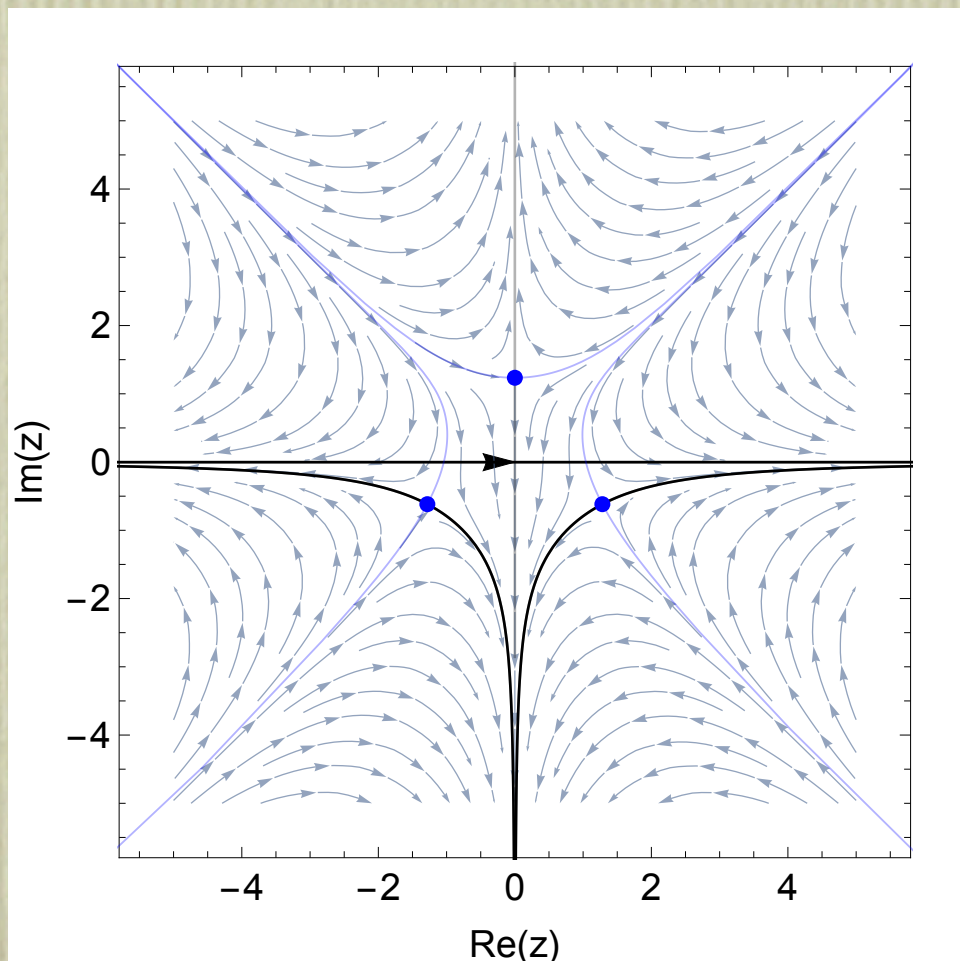
$$Z = \int_{-\infty}^{\infty} dx e^{-S(x)}$$

$$\frac{dS}{dz} = 0 \quad (\text{critical points})$$

$$\frac{dz}{d\tau} = \overline{\frac{\partial S}{\partial z}}, \quad z \equiv x + iy$$

$$\begin{cases} \frac{dx}{d\tau} = \frac{\partial S_R}{\partial x} = \frac{\partial S_I}{\partial y} \\ \frac{dy}{d\tau} = \frac{\partial S_R}{\partial y} = -\frac{\partial S_I}{\partial x} \end{cases}$$

Holomorphic gradient flow and Lefschetz thimbles



$$Z = \sum_{\sigma} n_{\sigma} \int_{J_{\sigma}} dz e^{-S(z)}$$

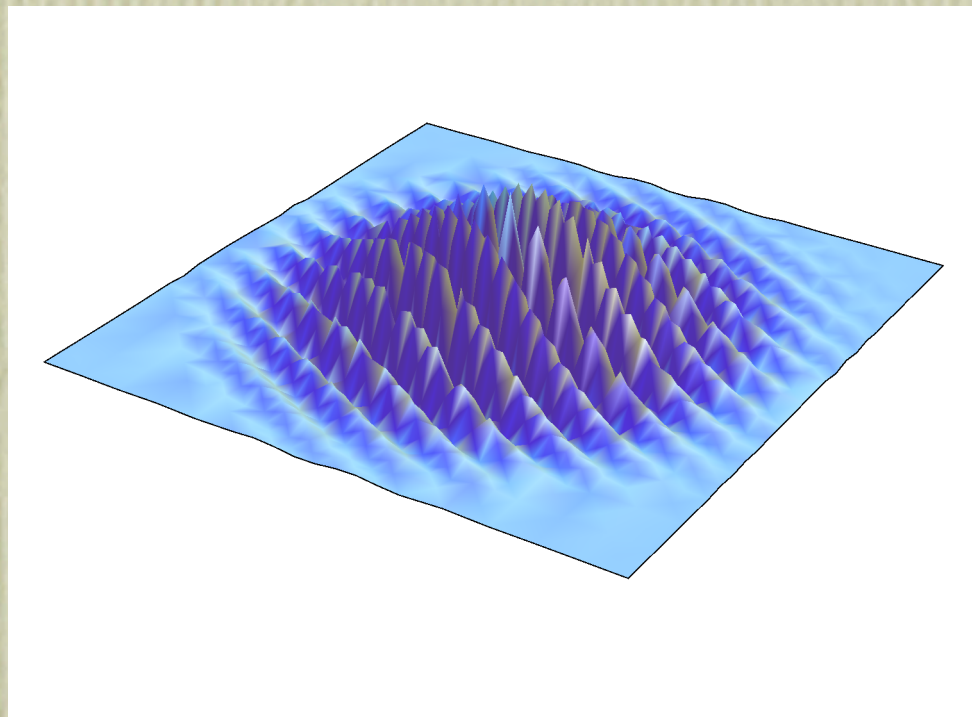
$$Z = \int_{-\infty}^{\infty} dx e^{-S(x)}$$

$$\frac{dS}{dz} = 0 \quad (\text{critical points})$$

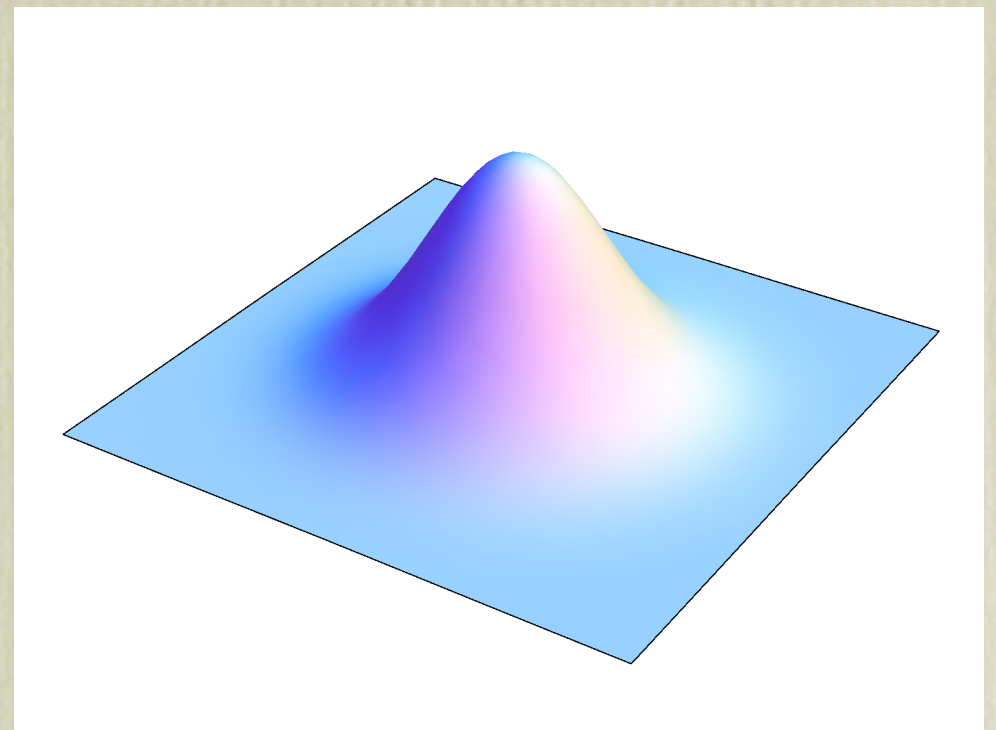
$$\frac{dz}{d\tau} = \overline{\frac{\partial S}{\partial z}}, \quad z \equiv x + iy$$

$$\begin{cases} \frac{dx}{d\tau} = \frac{\partial S_R}{\partial x} = \frac{\partial S_I}{\partial y} \\ \frac{dy}{d\tau} = \frac{\partial S_R}{\partial y} = -\frac{\partial S_I}{\partial x} \end{cases}$$

Lefschetz thimble



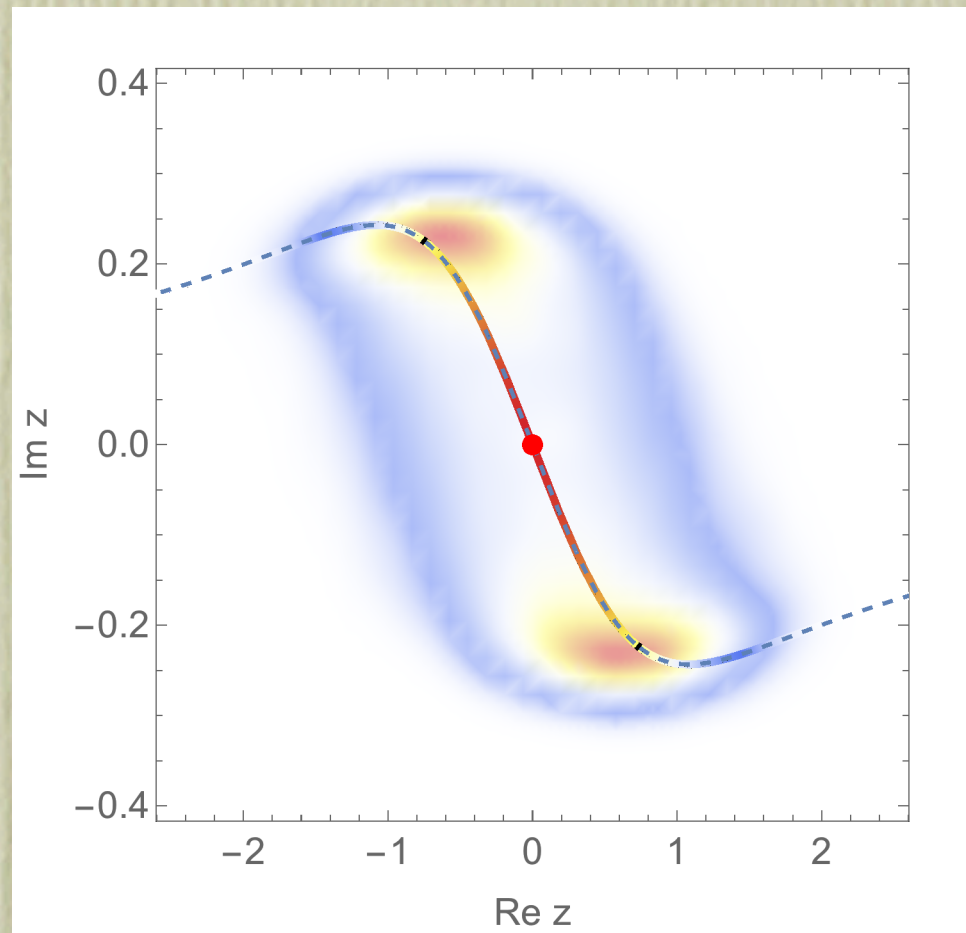
$$e^{-S(x_1, x_2)} \quad (\text{real plane})$$



$$e^{-S(z_1, z_2)} \quad (\text{gaussian thimble})$$

$$S(x_1, x_2) = x_1^2 + x_2^2 + 10ix_1 + 20ix_2 + ix_1x_2/3$$

Complex Langevin vs contour deformation



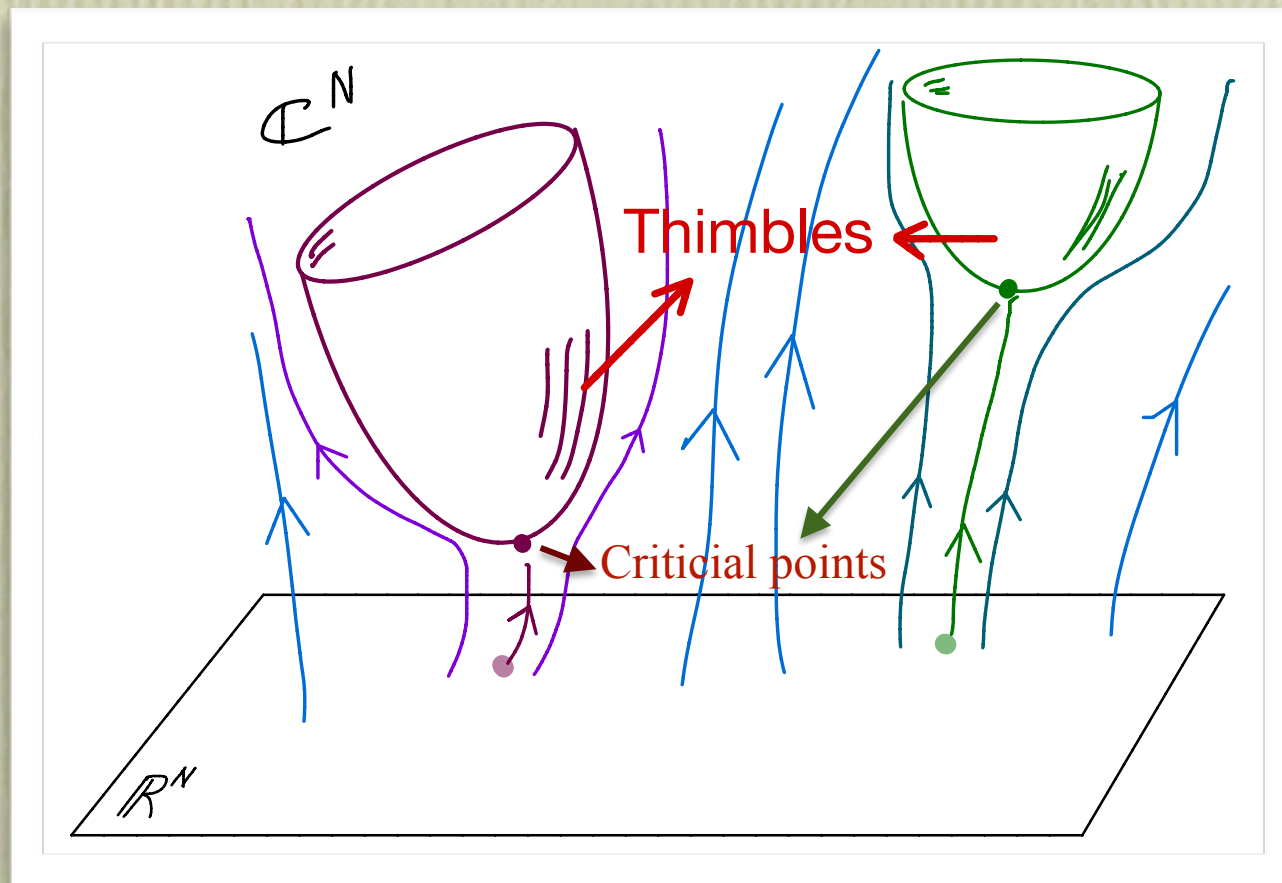
$$S(z) = \frac{1}{2}(1+i)z^2 + \frac{1}{4}z^4$$

- Complex Langevin follows the stochastic differential equation

$$\dot{z} = -\partial_z S(z) + \eta$$

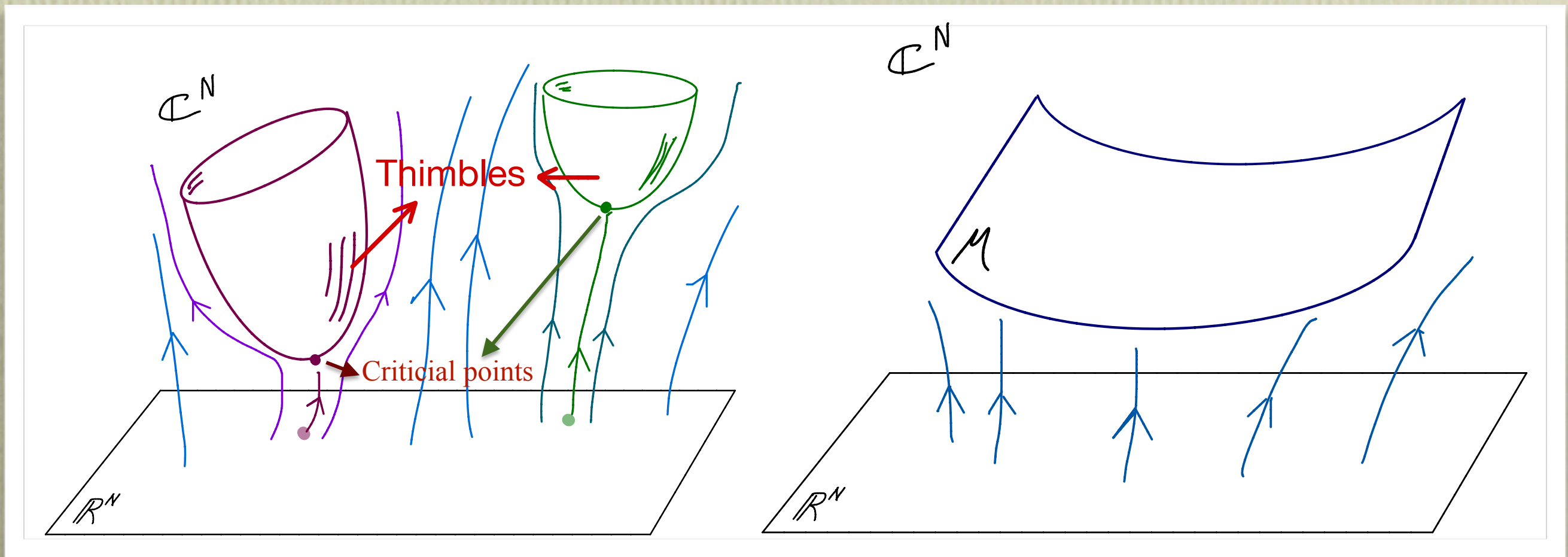
- The process moves freely in the complex plane with possible runaways
- Complex integration is constrained on a manifold of similar dimension with the original integration contour

Generalized thimble method



- Most systems require multiple thimble
- Thimble decomposition is hard
- Use the manifolds generated by the holomorphic flow

Manifolds generated by holomorphic gradient flow

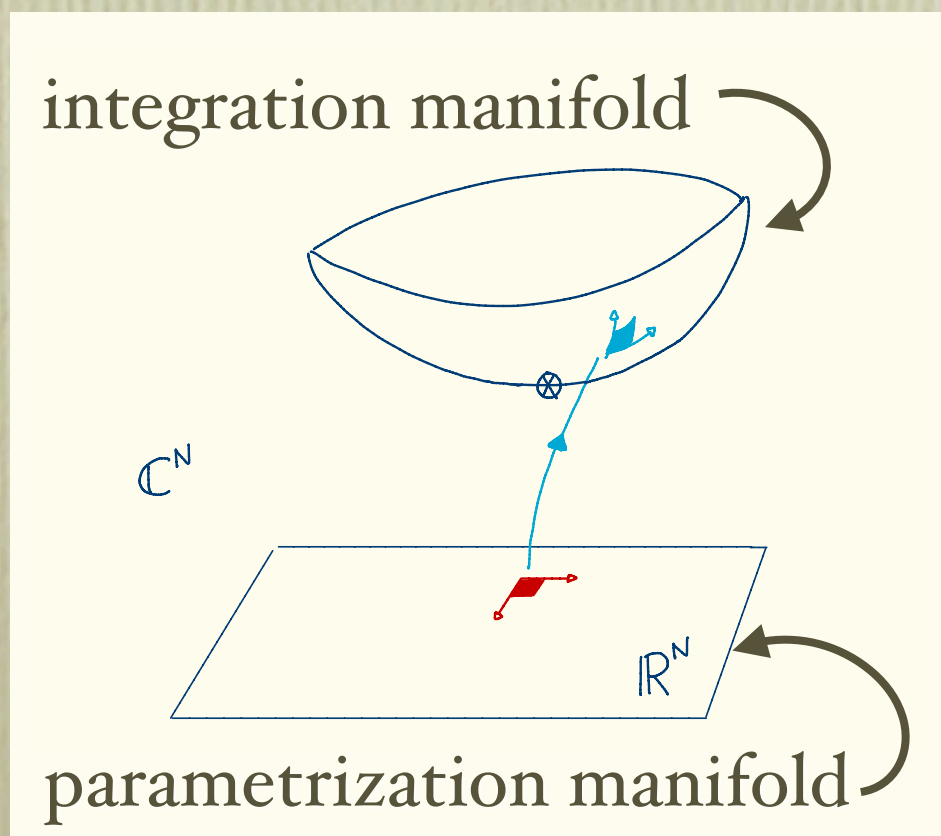


$$T_{\text{flow}} \rightarrow \infty \quad \Rightarrow \quad \mathcal{M} \rightarrow \text{sum over thimbles}$$

Basic idea

$$Z = \int_{\mathcal{M}} d^N z e^{-S(z)} = \int_{\mathbb{R}^N} d^N x \underbrace{\left\| \frac{\partial z_i}{\partial x_j} \right\|}_{\det J(x)} e^{-S(z(x))}$$

$$\langle \mathcal{O}(z) \rangle = \frac{1}{Z} \int_{\mathbb{R}^N} d^N x \underbrace{|\det J e^{-S(z(x))}|}_{e^{-S_{\text{eff}}(x)}} \Phi(x) \mathcal{O}(z(x)) = \frac{\langle \mathcal{O}(z(x)) \Phi(x) \rangle_{S_{\text{eff}}}}{\langle \Phi(x) \rangle_{S_{\text{eff}}}}$$

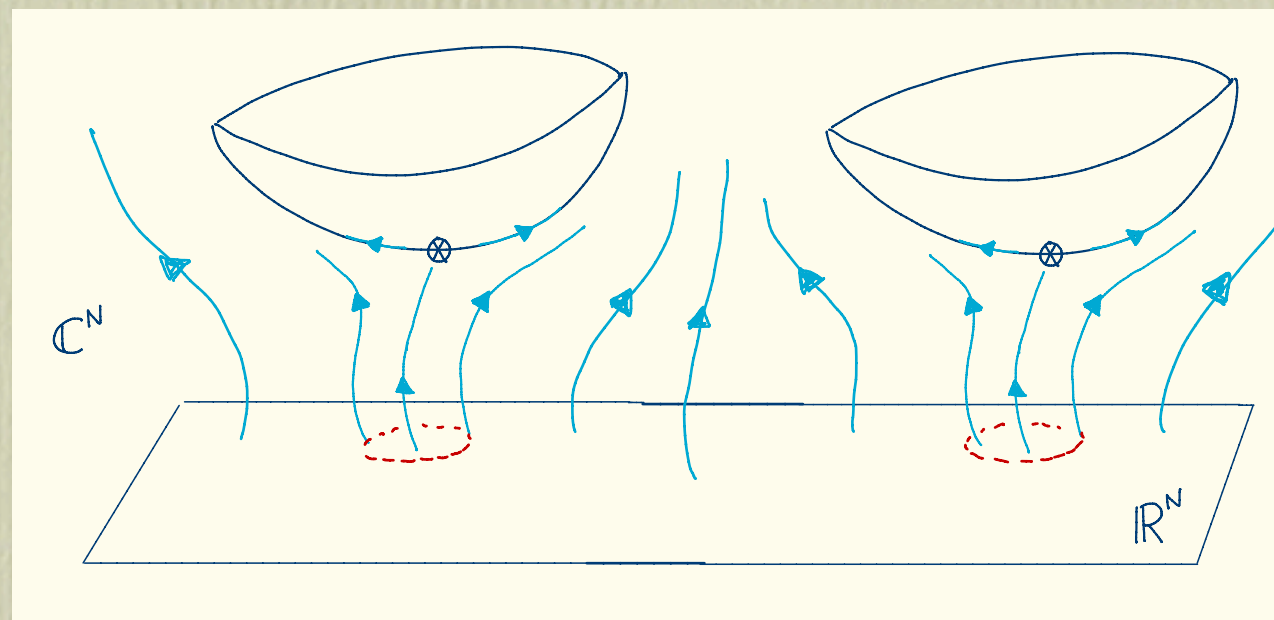


$$S_{\text{eff}}(x) = S_R(z(x)) - \ln |\det J(x)|$$

$$\Phi(x) = e^{i[S_I(z(x)) - \text{Im} \det J(x)]}$$

$$J_{ij} = \frac{\partial z_i}{\partial x_j}$$

Manifolds generated by holomorphic gradient flow



- Small regions are mapped (close) to thimbles and contribute significantly to the integral, S_I varies little.
- The other regions flow towards $S_{R=\infty}$ and contribute little to the integral.

Case study: massive Thirring model in 1+1D

$$\mathcal{L} = \bar{\psi}^a (\gamma^\mu \partial_\mu + m + \mu \gamma^0) \psi^a + \frac{g^2}{2N_f} (\bar{\psi}^a \gamma^\mu \psi^a) (\bar{\psi}^b \gamma_\mu \psi^b)$$

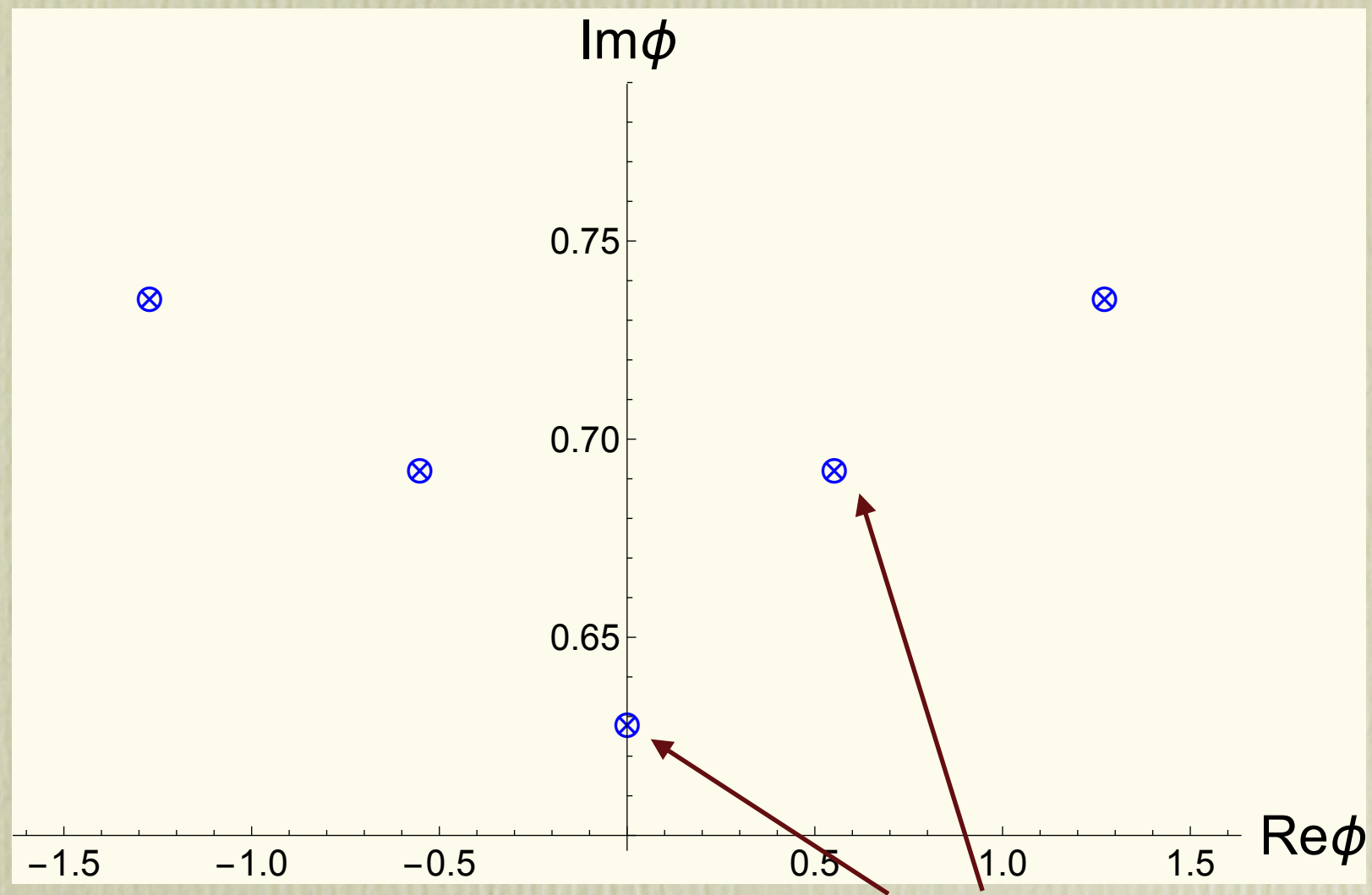
Auxiliary field A's

$$S = \int d^2x \left[\frac{N_F}{2g^2} A_\mu A_\mu + \bar{\psi}^\alpha (\not{\partial} + \mu \gamma_0 + i \not{A} + m) \psi^\alpha \right]$$

Discretization (compact A's)

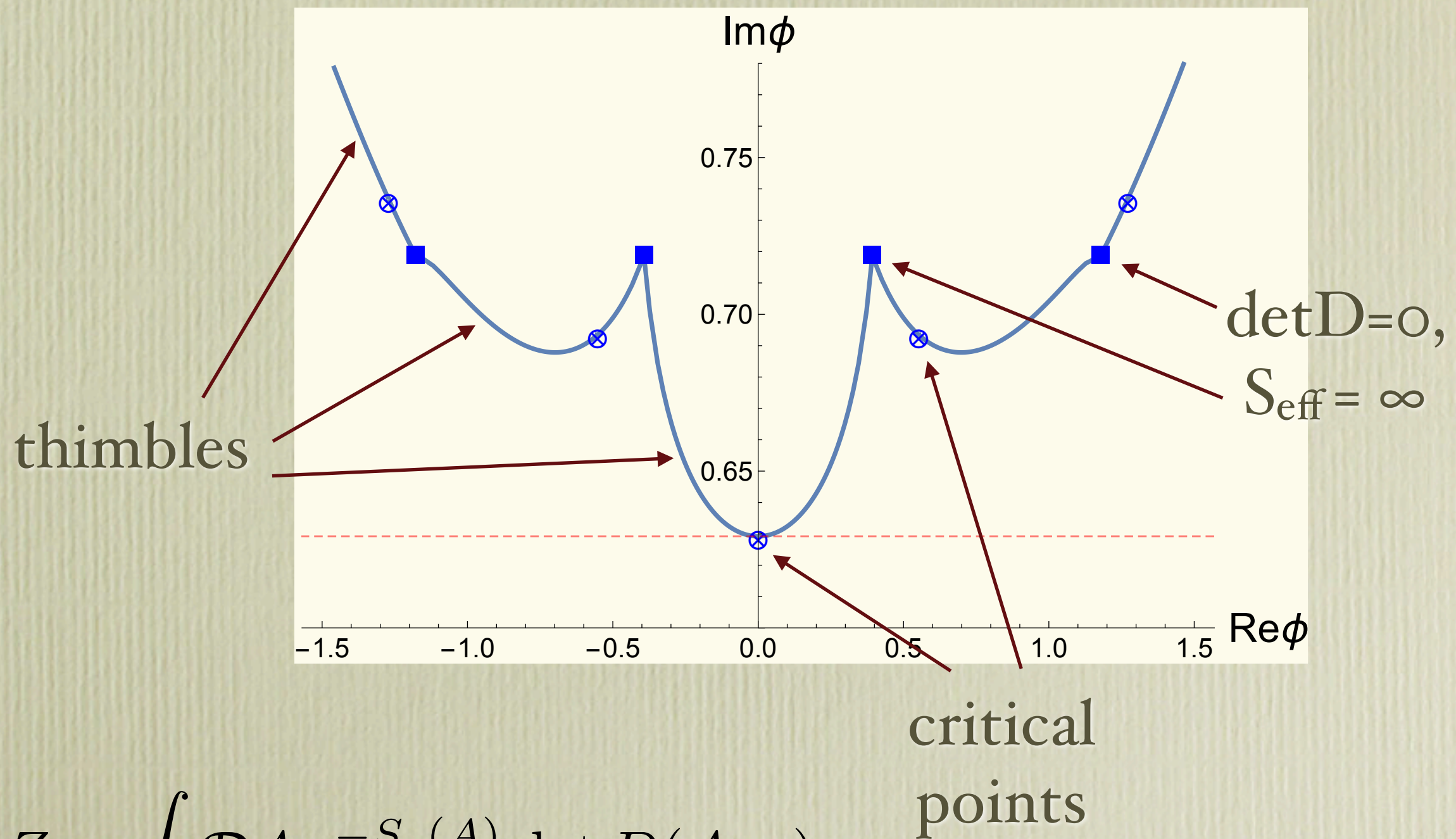
$$S = N_F \left(\frac{1}{g^2} \sum_{x,\nu} (1 - \cos A_\nu(x)) - \gamma \log \det D(A) \right)$$

A projection of the thimbles: $\phi = \frac{1}{L^2} \sum_x A_0(x)$



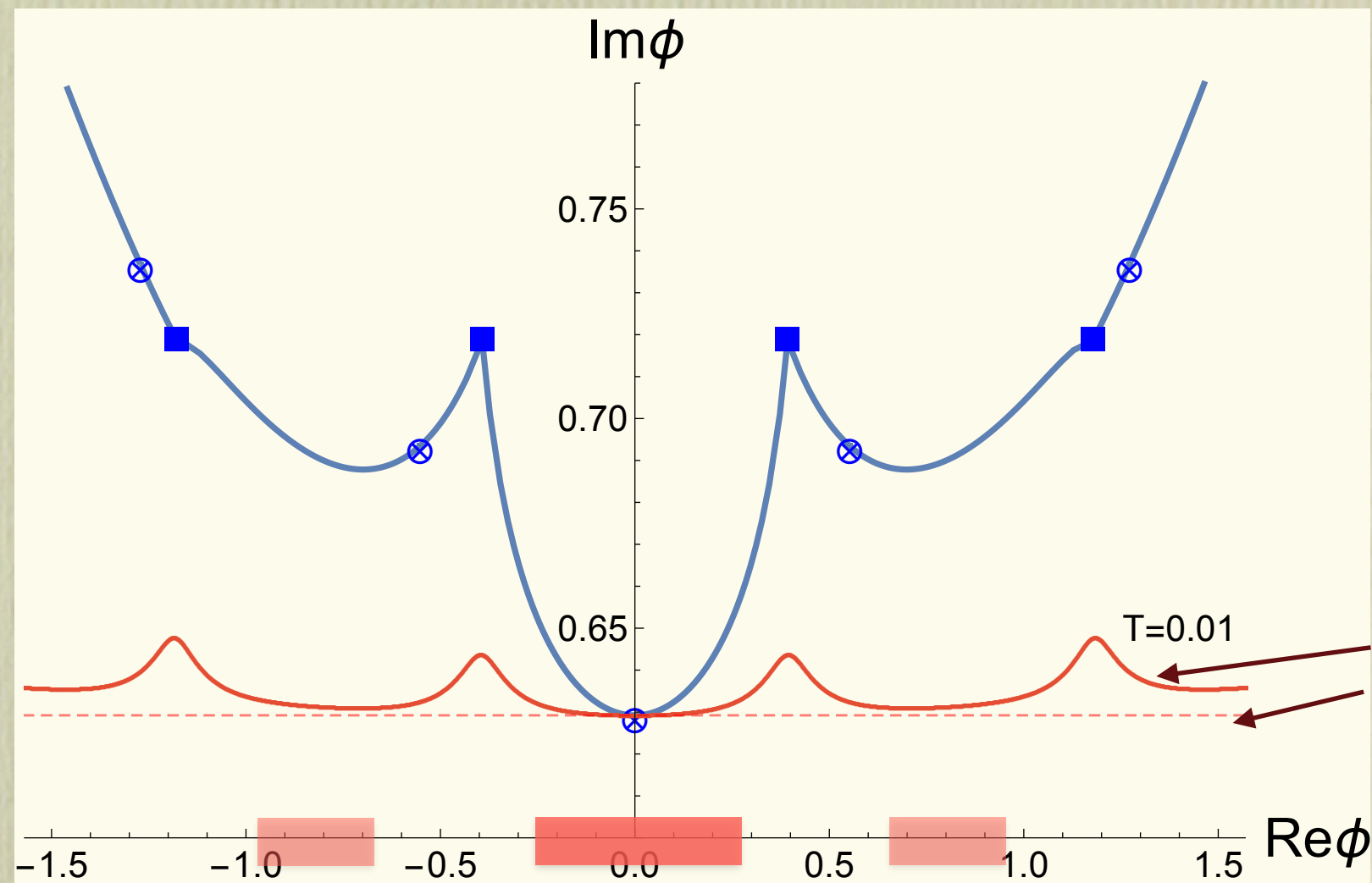
critical
points

A projection of the thimbles: $\phi = \frac{1}{L^2} \sum_x A_0(x)$



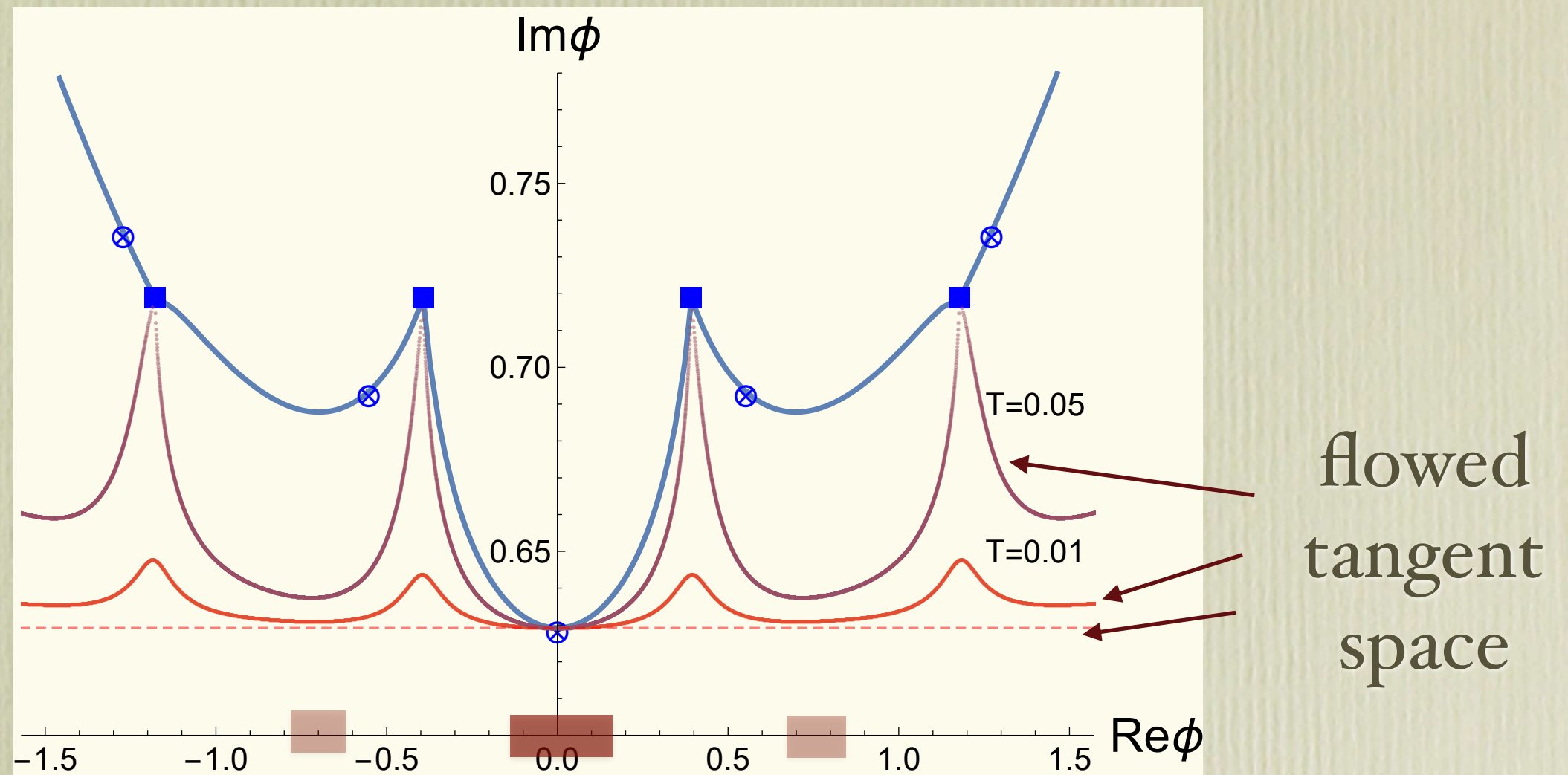
$$Z = \int \mathcal{D}A e^{-S_g(A)} \det D(A, \mu)$$

A projection of the thimbles: $\phi = \frac{1}{L^2} \sum_x A_0(x)$

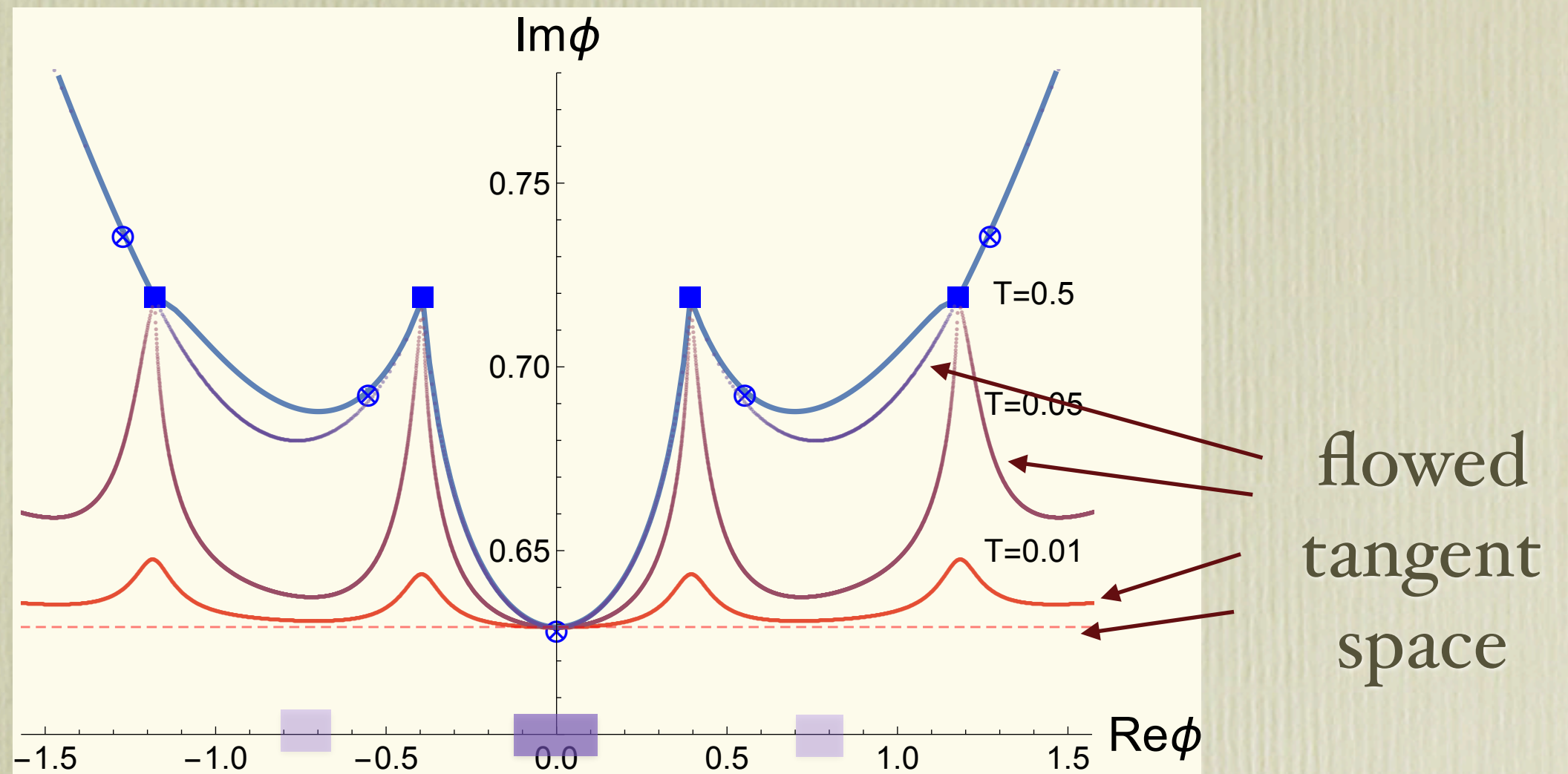


same
homological
class

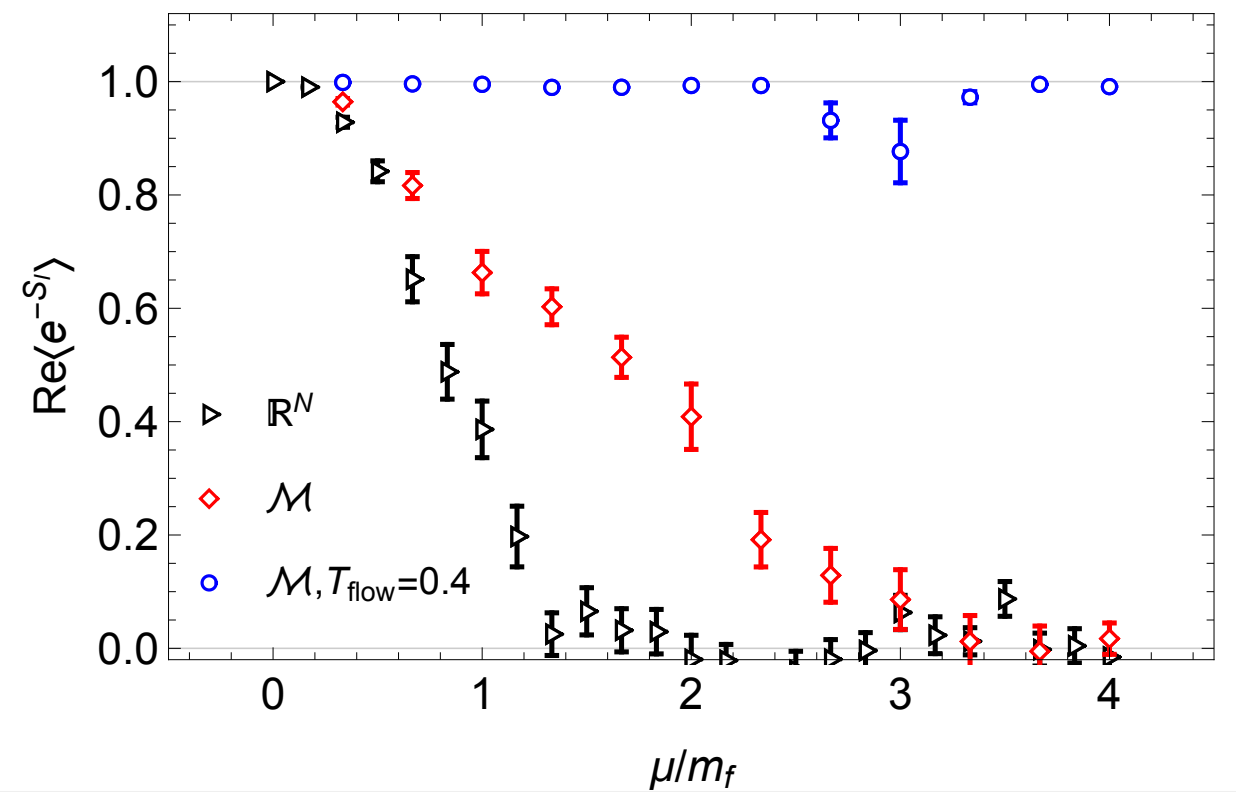
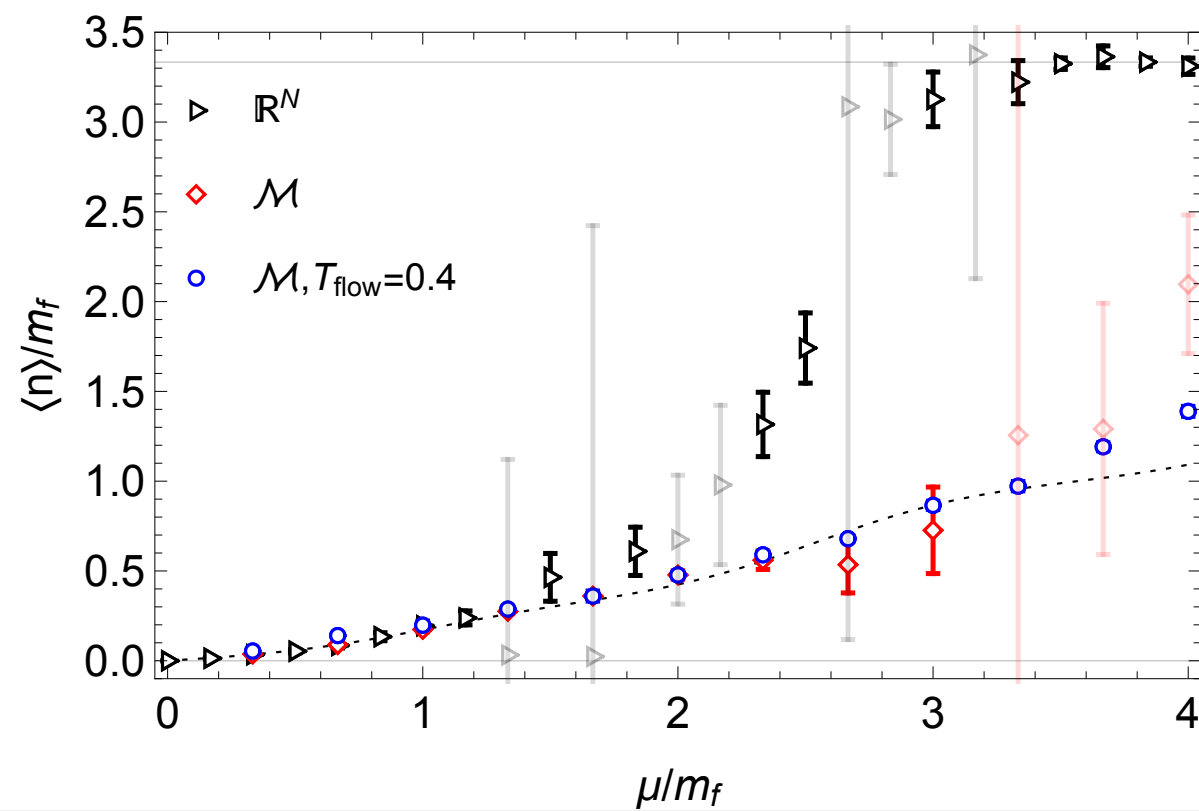
A projection of the thimbles: $\phi = \frac{1}{L^2} \sum_x A_0(x)$



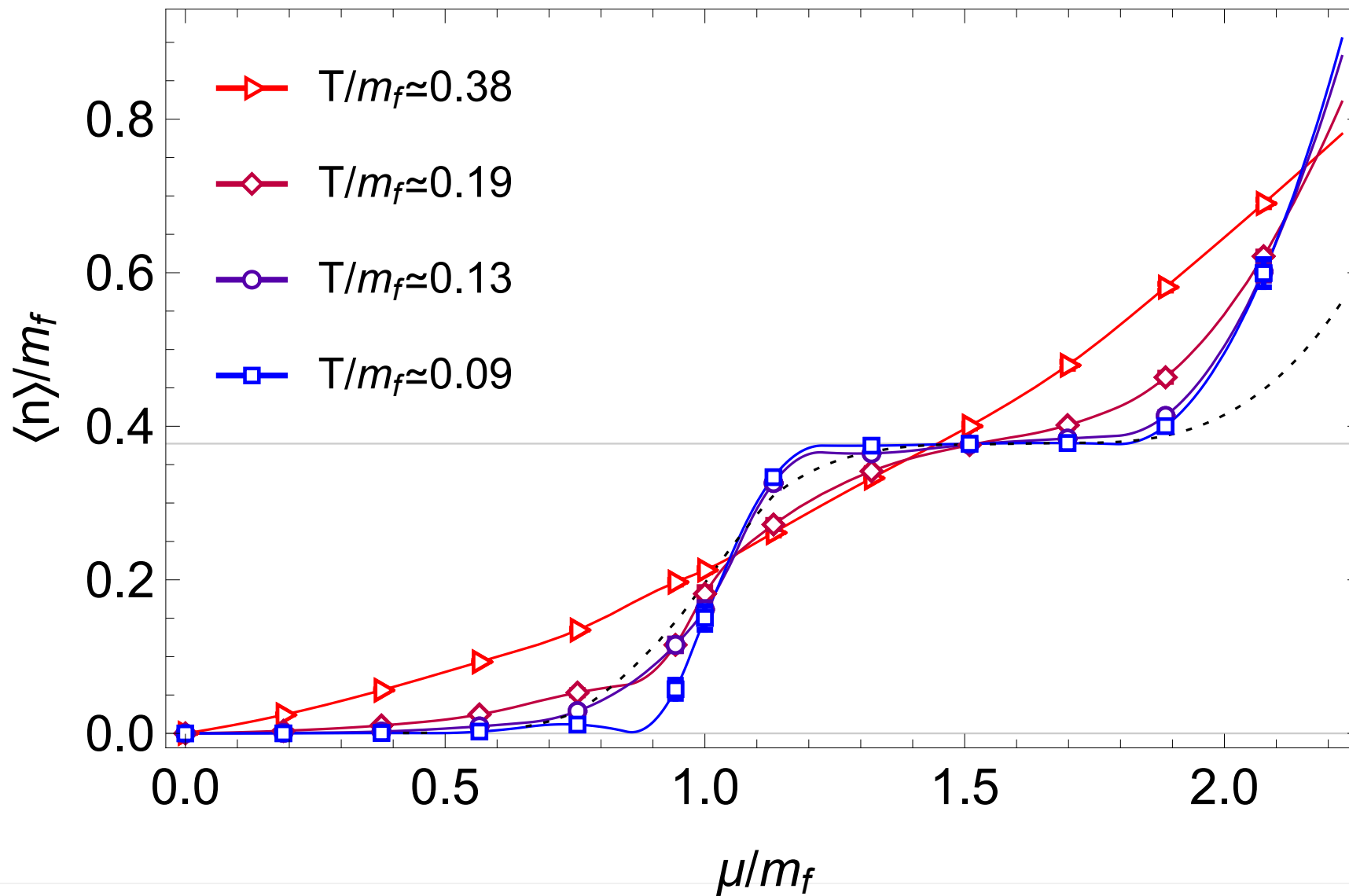
A projection of the thimbles: $\phi = \frac{1}{L^2} \sum_x A_0(x)$



Sign problem



Silver blaze (cold limit)

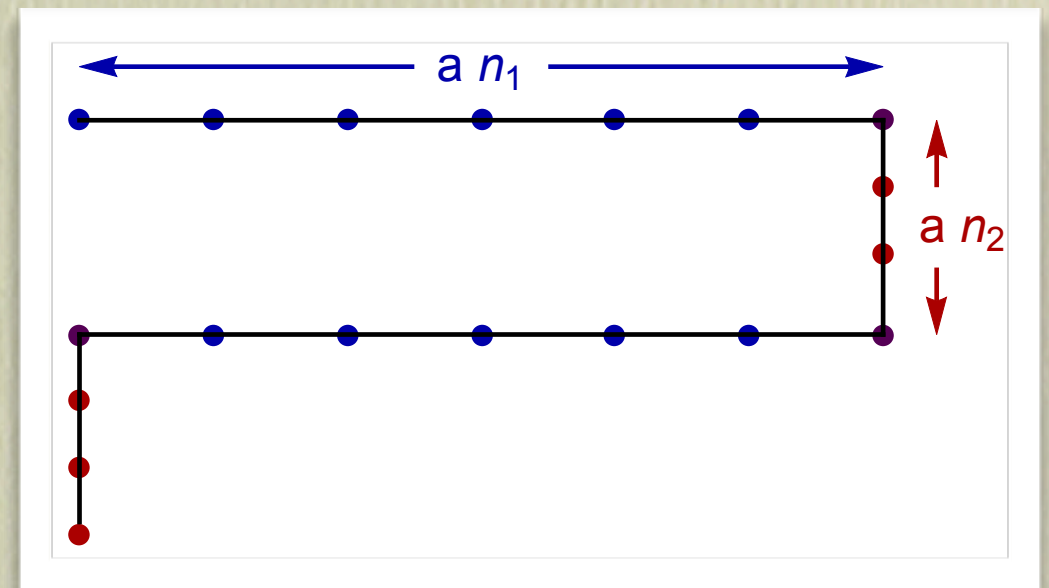
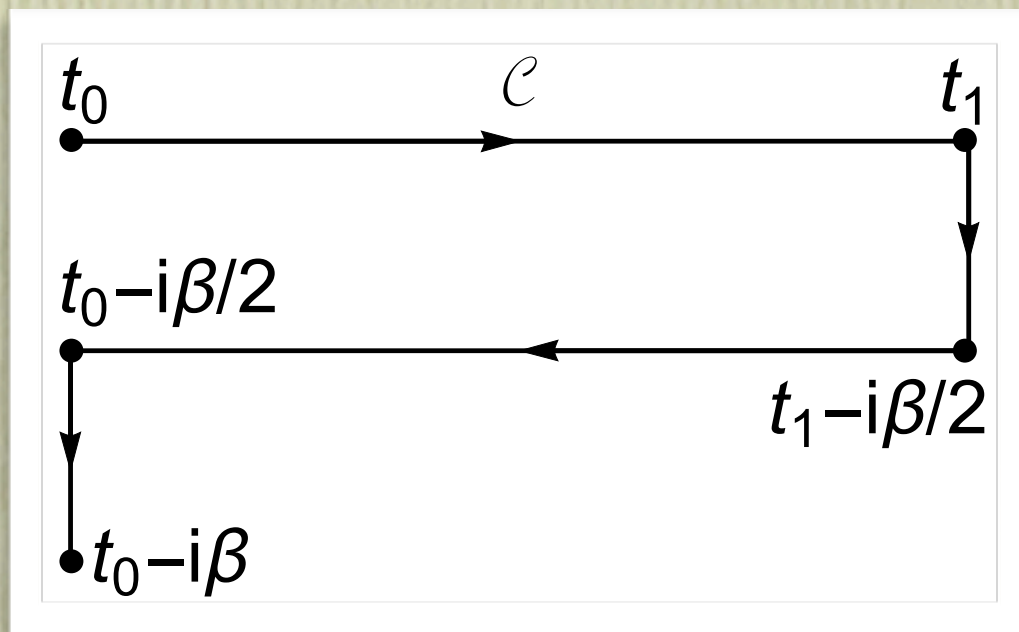


Case study: real time physics

- Motivation: compute out-of-equilibrium correlators, transport coefficients non-perturbatively from first principles
- Observables of interest are transport coefficient such as shear viscosity, conductivity, etc.
- At thermal equilibrium the observables are of the type

$$\langle \mathcal{O}_1(t) \mathcal{O}_2(t') \rangle = \text{Tr}[\mathcal{O}_1(t) \mathcal{O}_2(t') \hat{\rho}], \quad \hat{\rho} = e^{-\beta H}$$

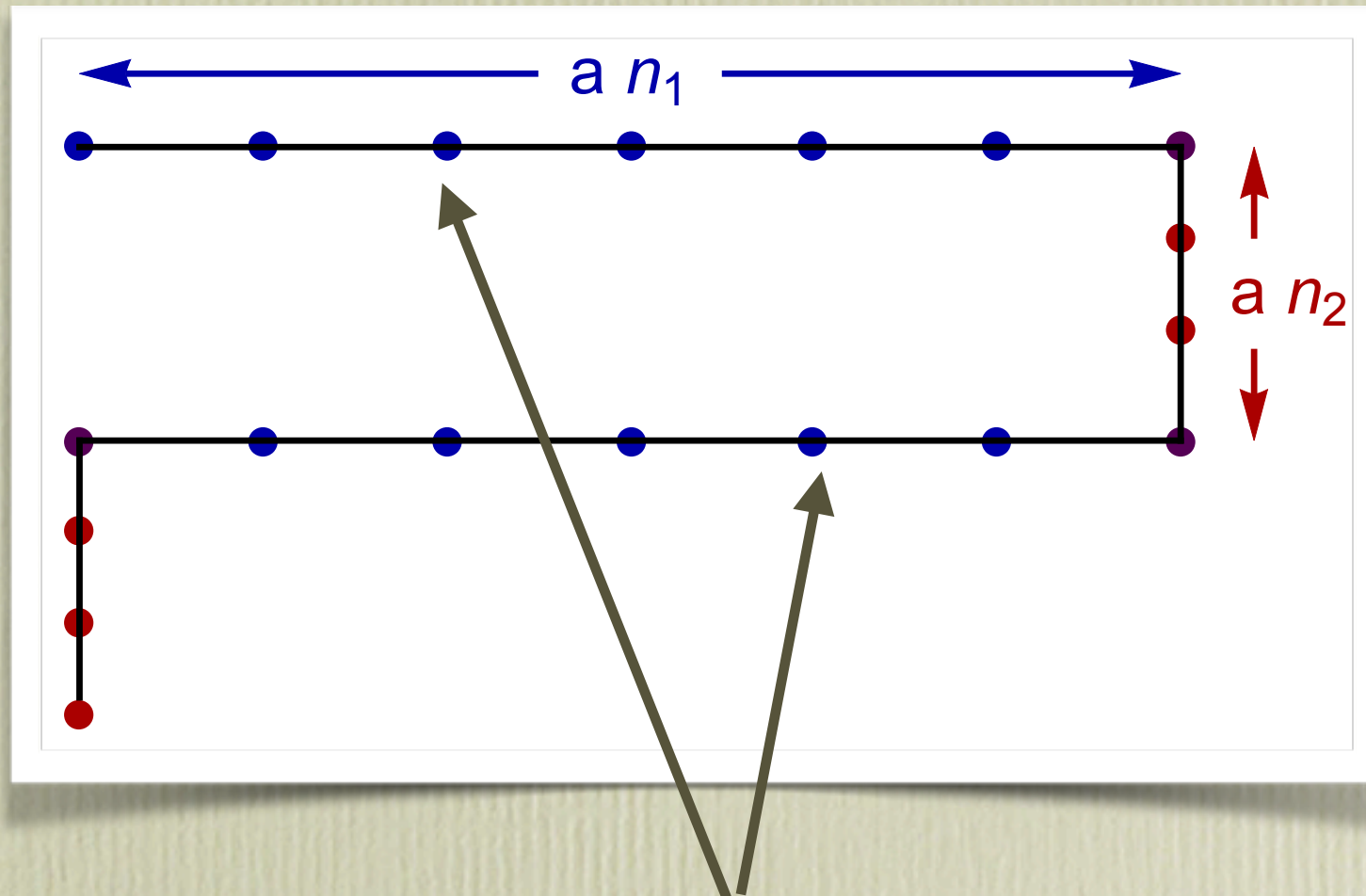
Real time physics



$$S_{SK}[\phi] = iS[\phi] = \int_C dt L[\phi] \quad \langle \mathcal{O}_1(t) \mathcal{O}_2(t') \rangle = \frac{1}{Z} \int \mathcal{D}\phi e^{-S[\phi]} \mathcal{O}_1(t) \mathcal{O}_2(t')$$

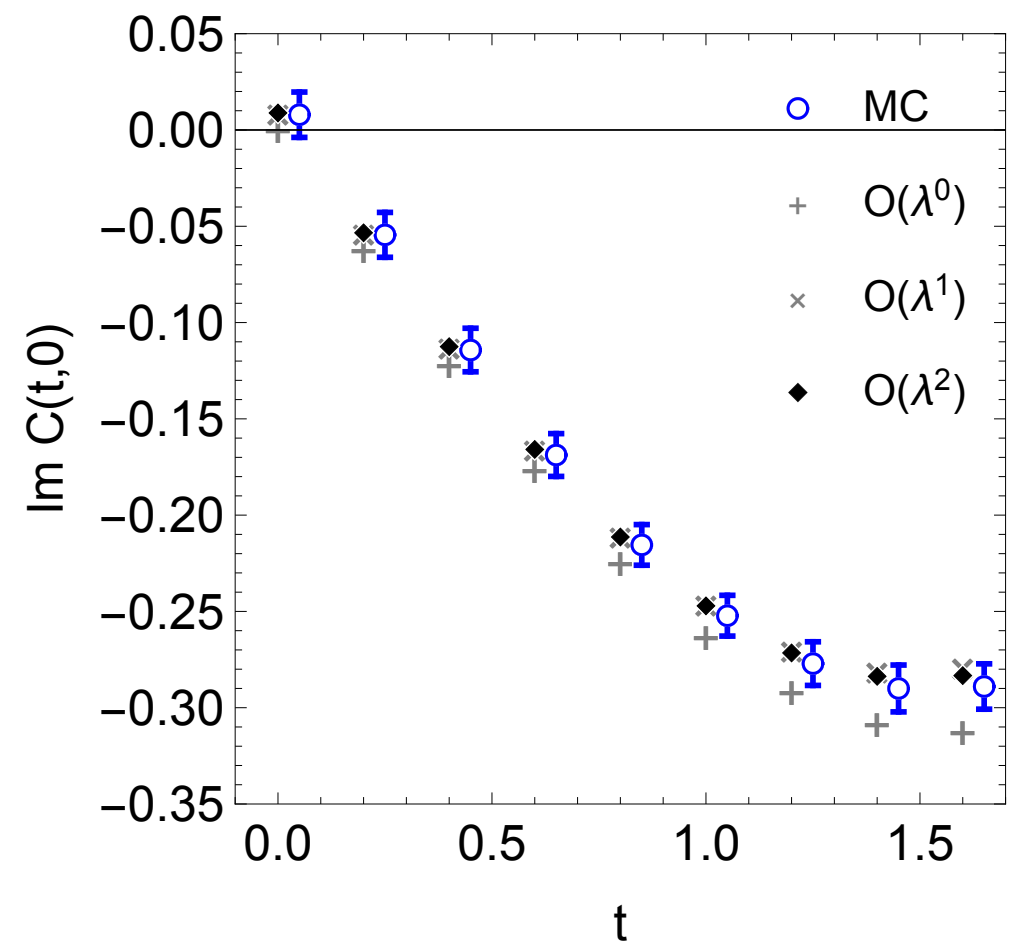
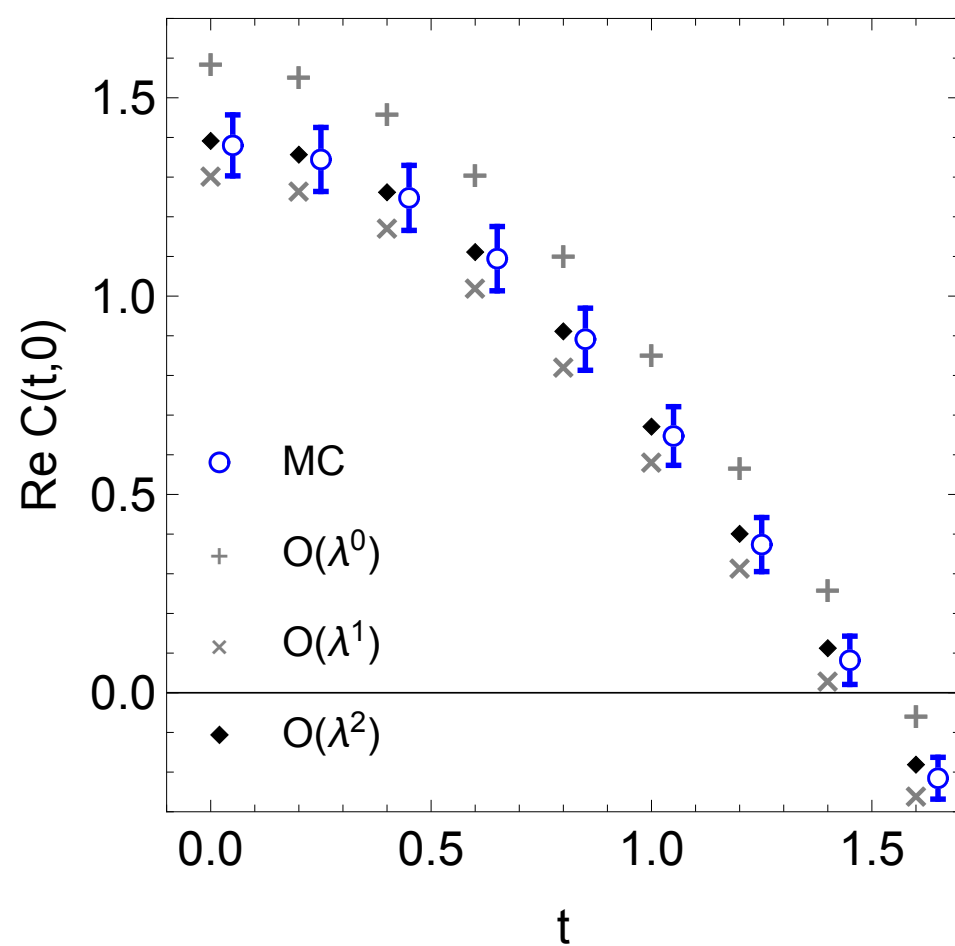
$$S[\phi] = \sum_{t,n} a_t a \left[\frac{(\phi_{t+1,n} - \phi_{t,n})^2}{2a_t^2} + \frac{1}{2} \left(\frac{(\phi_{t+1,n+1} - \phi_{t+1,n})^2}{2a^2} + \frac{(\phi_{t,n+1} - \phi_{t,n})^2}{2a^2} \right) \right. \\ \left. + \frac{1}{2} m^2 \frac{\phi_{t,n}^2 + \phi_{t+1,n}^2}{2} + \frac{\lambda}{4!} \frac{\phi_{t+1,n}^4 + \phi_{t,n}^4}{2} \right]$$

The worst sign problem



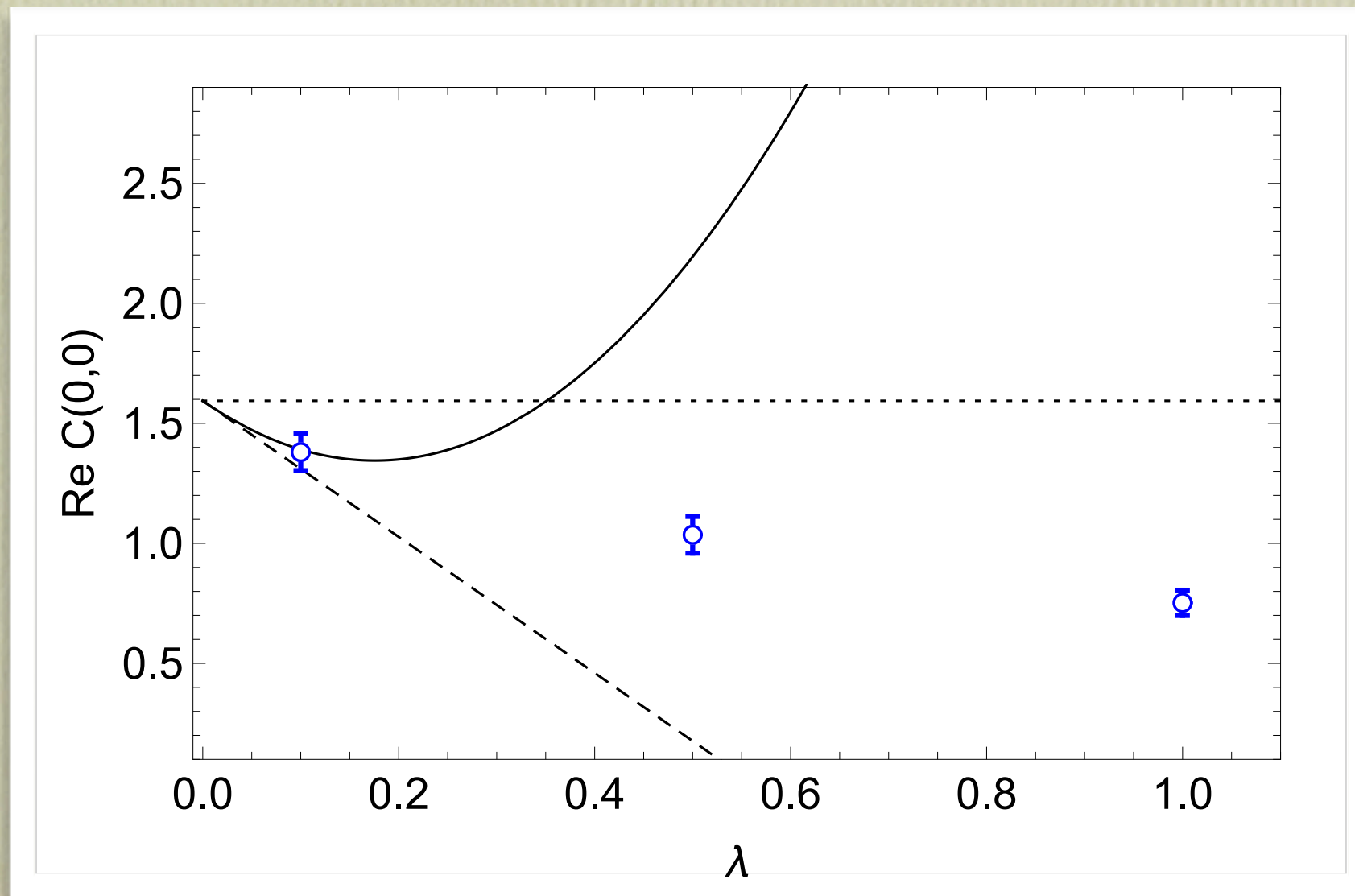
The field variables attached to real time legs contribute a purely imaginary factor to the action because $\exp(-a S_n) = \langle \phi_{n+1} | \exp(-iaH) | \phi_n \rangle$ produces a contribution to the action S_n that is purely imaginary.

Real time physics (1+1D) weak coupling

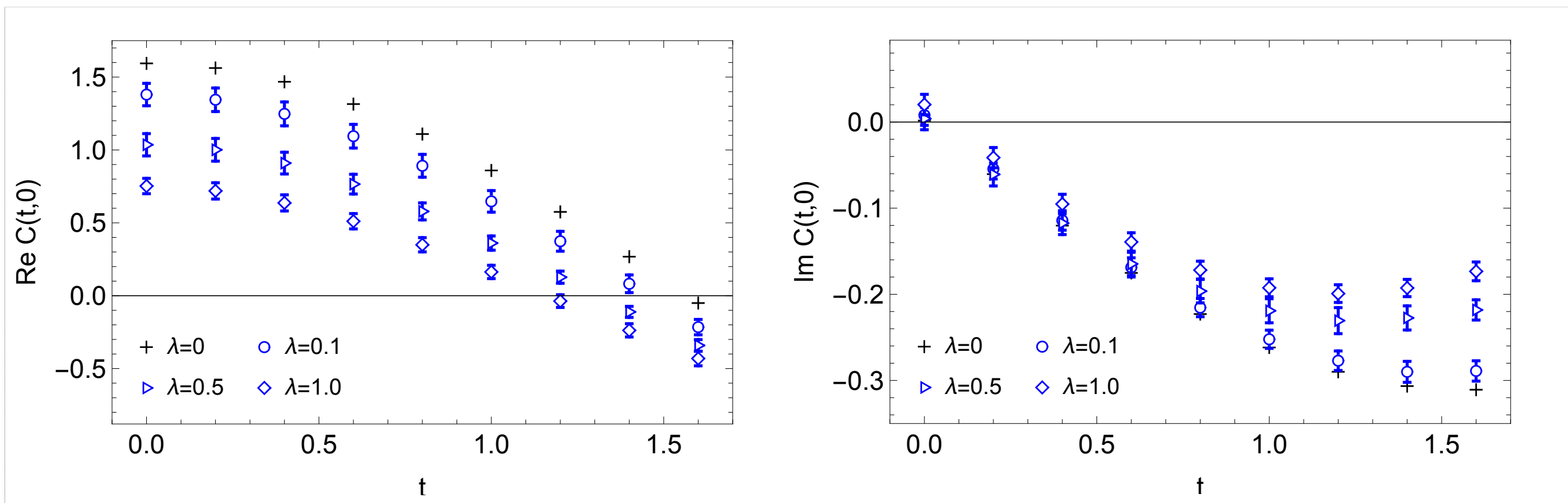


1+1D ϕ^4 : $n_t=8, n_x=8, n_\beta=2, \lambda=0.1$

Real time physics (I+ID) perturbation theory



Real time physics (1+1D) strong coupling



1+1D φ^4 : $n_t=8, n_x=8, n_\beta=2, \lambda=0.1, 0.5, 1.0$

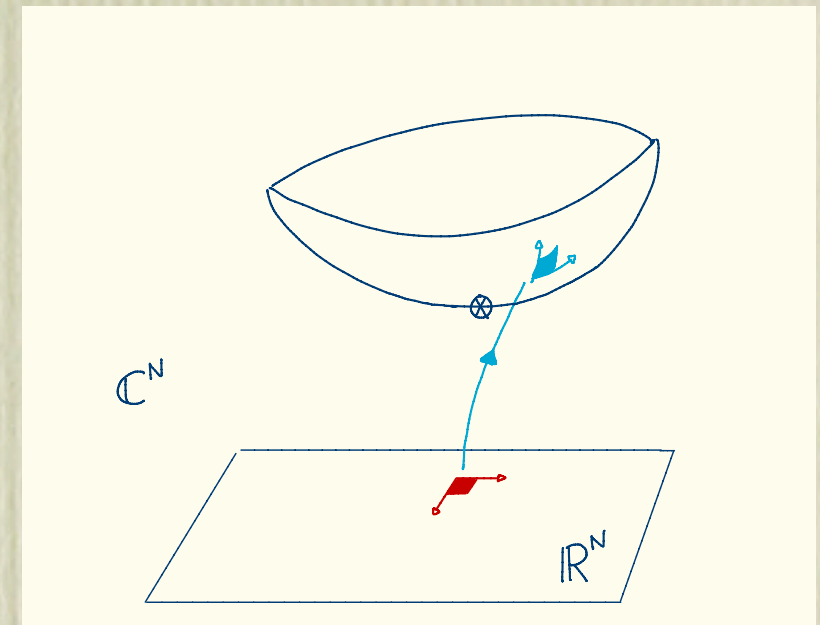
New directions

- On the flow manifolds sampling is done based on the effective action

$$S_{\text{eff}}(x) = S_R(z(x)) - \ln |\det J(x)|$$

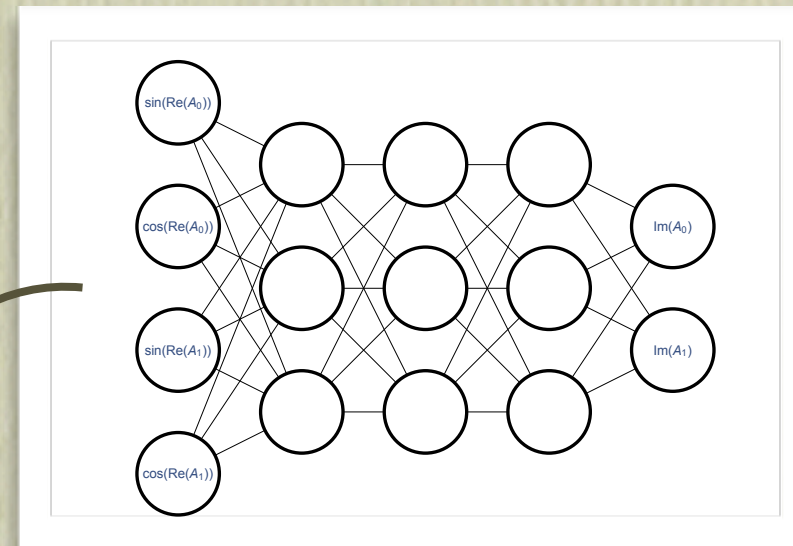
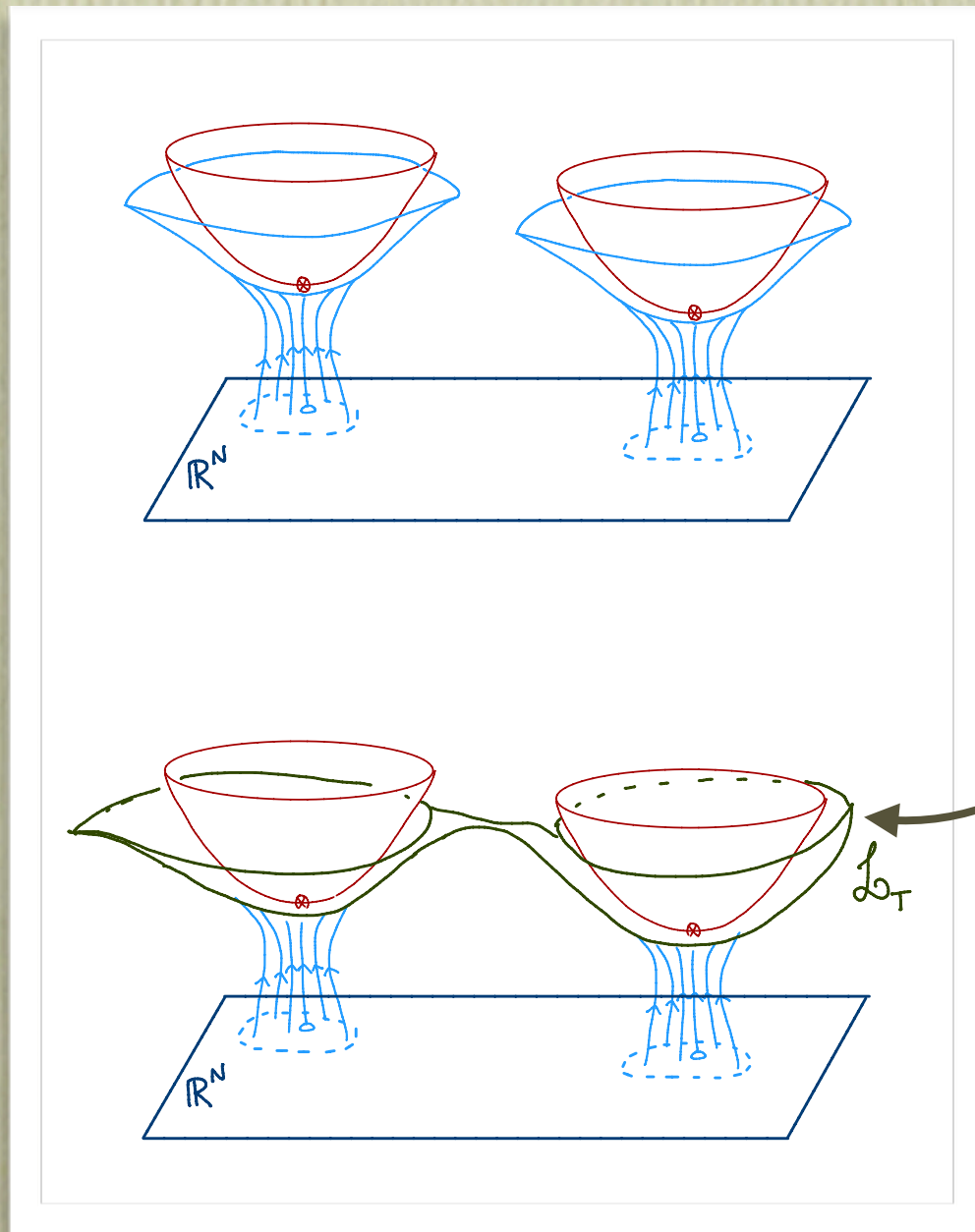
$$\frac{dz}{d\tau} = \overline{\frac{dS}{dz}}, \quad z(0) = x$$

$$\frac{dJ}{d\tau} = \overline{H(z)J}, \quad J(0) = I \quad H(z)_{ij} = \frac{\partial^2 S}{\partial z_i \partial z_j}$$



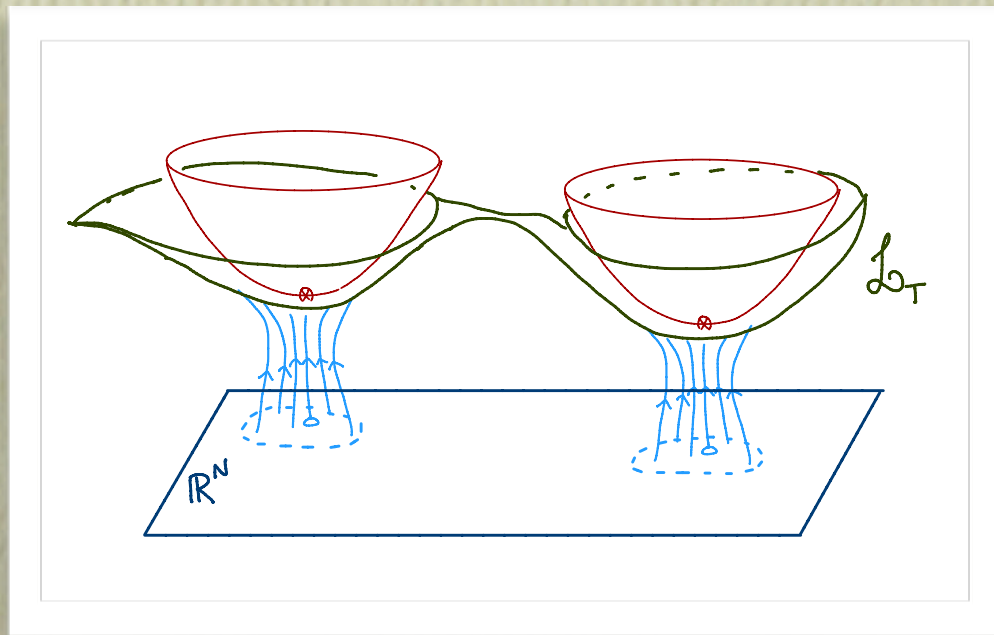
- For each step integrate a set of differential equations to get z and J
- This is expensive, especially the calculation of J and $\det J$
- To address this problem we used
 - improved sampling algorithms (avoid computing J or $\det J$)
 - fast estimators for $\det J$
 - **numerically cheaper integration manifolds**

New directions — learnifold

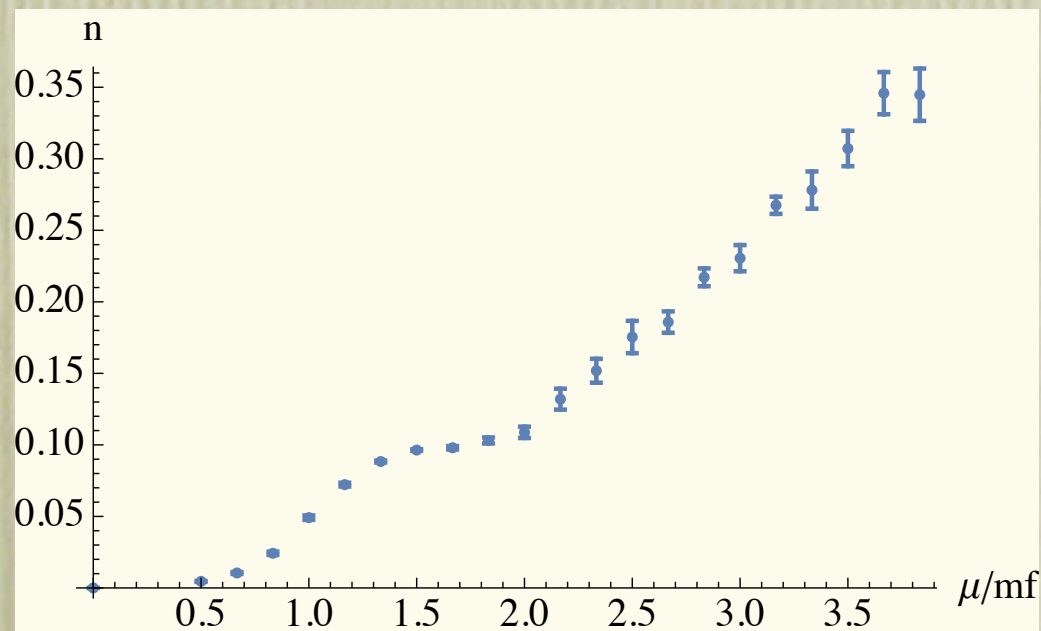


- Generate few configs on the integration manifold
- Use neural nets with appropriate symmetries to interpolate
- Integrate over the learnifold, the manifold defined by the trained neural net

New directions — learnifold



Wilson, 20×10 lattice, $NF=2$, $am_f=0.3$

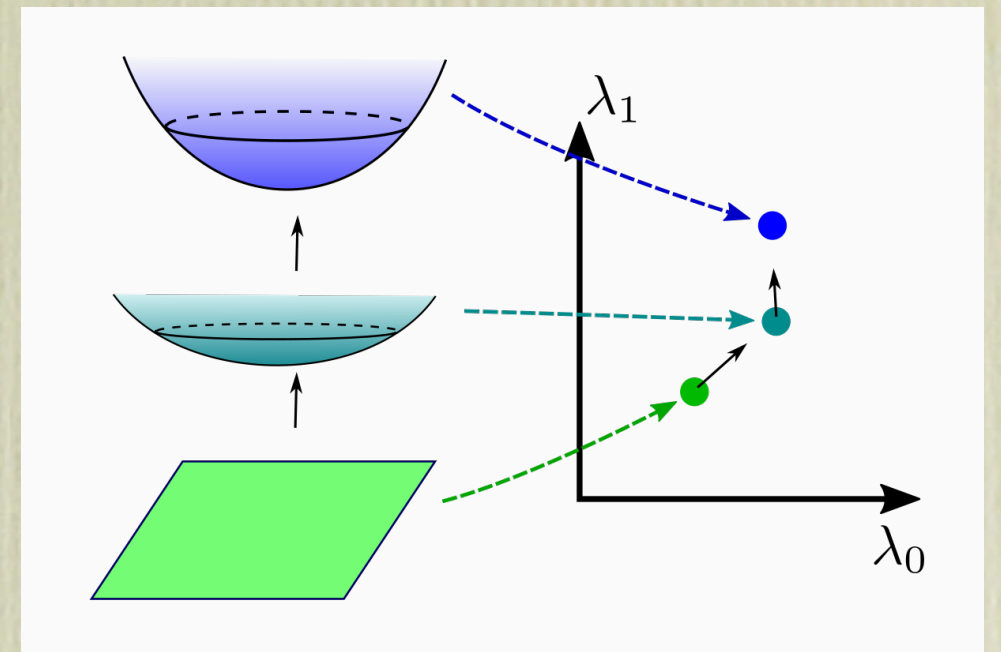


- We use a feed-forward network and train it using supervised learning
- The network learns quickly about the constant shift, further improvements are slow
- Most of the cost is in generating the seed configurations with much less required for training
- Integrations over learnifold is fast and we were able to use it to explore larger parameter region for Thirring 1+1 model

Sign optimized manifolds

$$\langle \sigma \rangle = \frac{\int_{\mathcal{M}} dz e^{-S(z)}}{\int_{\mathcal{M}} dz e^{-S_R(z)}} = \frac{Z}{Z_{\text{pq}}}$$

Since $\nabla_{\lambda} Z = 0$ the sign average can be optimized by minimizing the **phase-quenched** partition function



For a given ansatz $z = f_{\lambda}(x)$ we can maximize $\langle \sigma \rangle$ with respect to λ , using a stochastic gradient descent. For a well chosen ansatz, the estimate for the gradient can be computed quickly.

$$\nabla_{\lambda} \log \langle \sigma \rangle = \langle \nabla_{\lambda} S - \text{Tr} \log J^{-1} \nabla_{\lambda} J \rangle_{\text{Re} S_{\text{eff}}}$$

Sign optimized manifolds

- For Thirring model in 2+1 dimensions, we use an ansatz motivated by the dense limit

$$A_0(x) \rightarrow A_0(x) + i f_\lambda[A_0(x)]$$

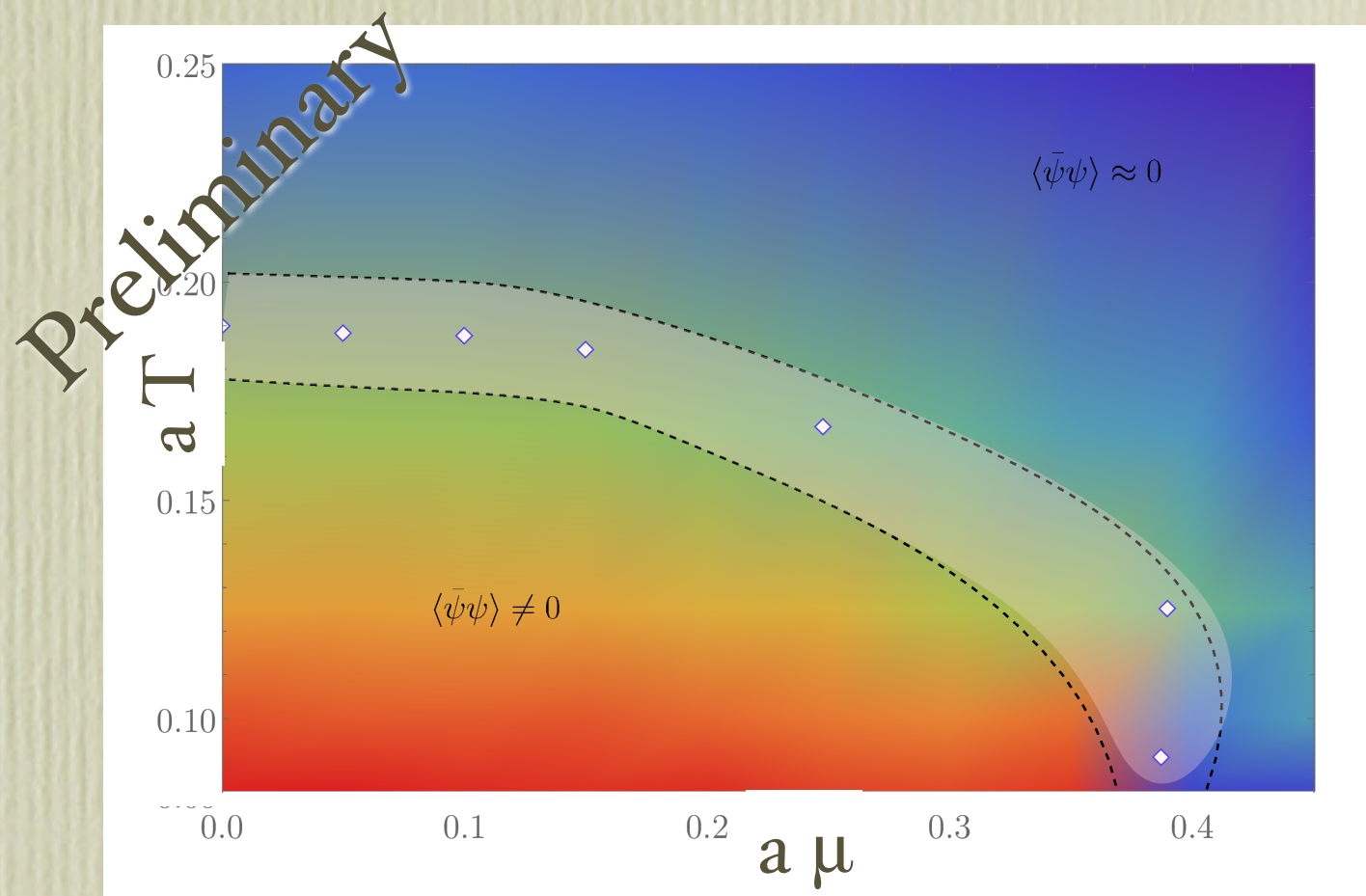
$$A_1(x) \rightarrow A_1(x)$$

$$f_\lambda(x) = \lambda_0 + \lambda_1 \cos x + \lambda_2 \cos 2x$$

- For this ansatz the Jacobian can be computed efficiently

$$\det J = \prod_x [1 + i f'(A_0(x))]$$

- We carry out the sign optimization for a set of temperatures and densities to investigate the phase diagram



Conclusions

- Complex manifold integration is a generic method for systems with sign problems: finite density QFTs, real time, etc.
- Field complexification serves as a knob to control the sign problem.
- Holomorphic gradient flow generates a continuous family of manifolds with improved sign average (with Lefschetz thimble decomposition a limiting case).
- Thimbles and holomorphic flow manifolds are only one option. There is a large degree of freedom in choosing complex deformations to address the numerical challenges specific to the system of interest (with new challenges and opportunities).

References

arXiv:1510.0325	arXiv:1512.0876	arXiv:1604.00956
arXiv:1605.08040	arXiv:1606.02742	arXiv:1609.01730
arXiv:1703.02414	arXiv:1703.06404	arXiv:1709.01971
arXiv:1804.00697	arXiv:1807.02027	arXiv:1808.xxxxx